VERTICAL DIFFERENCING OF THE PRIMITIVE EQUATIONS

A. Arakawa
Department of Atmospheric Sciences
University of California, Los Angeles, USA

1. INTRODUCTION

In this lecture I shall discuss some of the basic problems in vertical differencing of the primitive equations. Th use of the hydrostatic equation is the only major approximation in the primitive equations, as far as adiabatic frictionless processes are concerned. Consequently, horizontally propagating sound wave (the Lamb wave) and internal gravity waves are among the solutions of the equations, although vertically propagating sound waves are filtered.

In the quasi-geostrophic system, horizontal advections by geostrophic wind are the only nonlinear terms. In the primitive equations, however, there are additional nonlinear terms associated with the horizontal advection by non-geostrophic wind and with the vertical advection. In addition, it is generally attempted to incorporate a realistic topography of the earth's surface into the system as the lower boundary condition.

These situations make vertical (and horizontal) differencing of the primitive equations more difficult than that of the quasi-geostrophic system of equations. We must properly choose a vertical coordinate, a vertical grid structure, a vertical difference scheme satisfactory for all possible types of motion, the vertical extent of the model, and finally, vertical spacing and resolution of the grid.

2. MERITS AND DEMERITS OF EACH VERTICAL COORDINATE

Among other possibilities, the height z, the pressure p (or ℓnp), or the potential temperature θ (or $\ell n\theta$) can be used as the vertical coordinate; but various versions of the σ-coordinate (Phillips, 1957), in which the earth's surface is a coordinate surface, are most commonly used for the primitive equations. Kasahara (1975) and Sunqvist (1979) discussed the governing equations (and boundary conditions) for each of the above coordinates, as well as for a general vertical coordinate.

Each of the above vertical coordinates (see Fig. 1) has its own merits and demerits. Use of the σ-type coordinate makes the lower boundary condition very simple because $\dot{\sigma} \equiv d\sigma/dt = 0$ there. The expense we are paying for this simplification is a com-

plication of the pressure gradient force. In this type of coordinate, the pressure gradient force appears as the sum of the two terms that are of comparable magnitude and opposite sign near steep topography. Discretization errors, therefore, even when they are small in either term, can result in a larger error in the pressure gradient force. This problem is discussed on one of Mesinger's lectures.

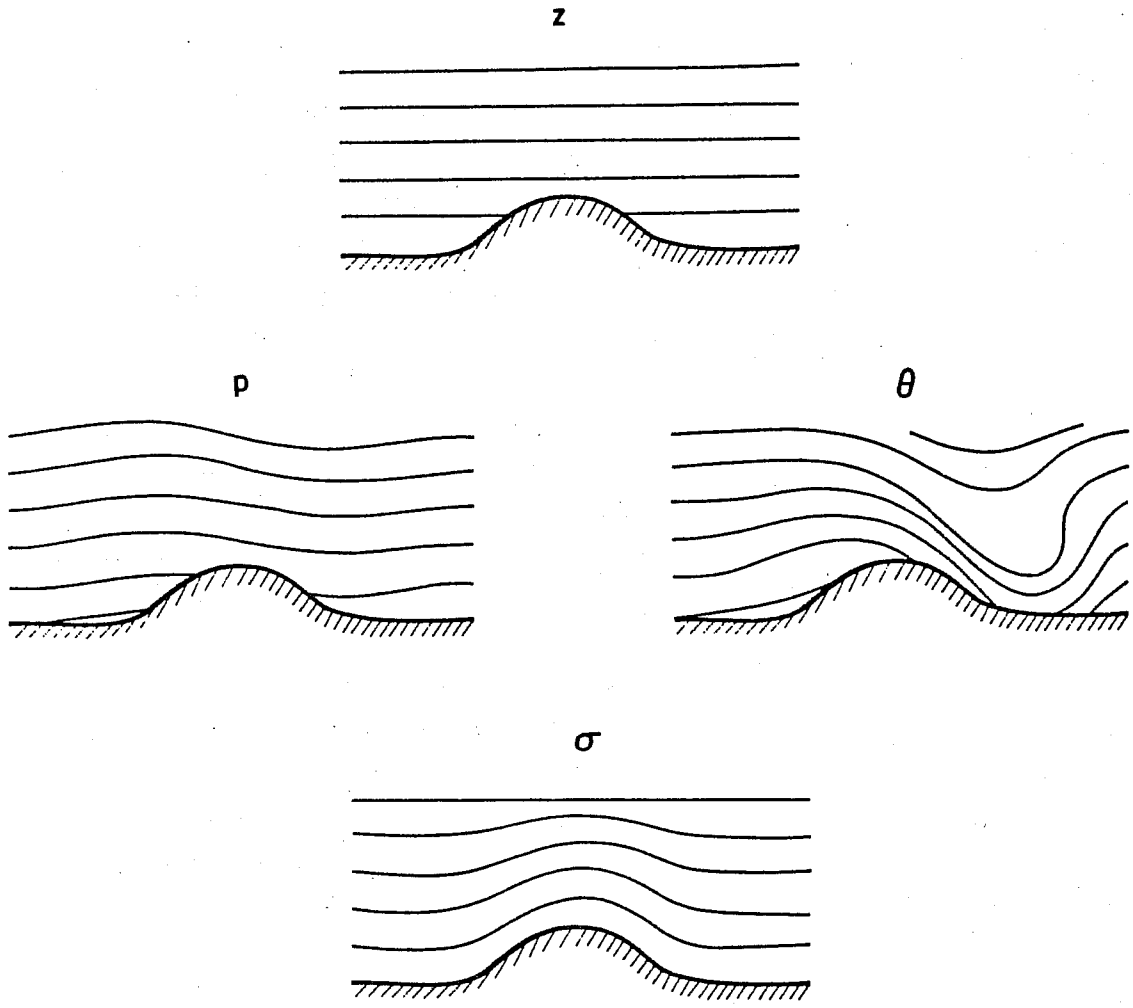

Fig. 1 Illustration of the heights of coordinate surfaces for the z-coordinate, the p-coordinate, the θ-coordinate and a σ-type coordinate.

The difficulty with a coordinate other than σ is that the coordinate surfaces can intersect the earth's surface and the lower boundary conditions must be incorporated in the form of the "lateral" boundary conditions. In addition, with the z-coordinate, the equation that diagnostically determines the vertical velocity (the Richardson equation) has a very awkward form unless the local time derivative of the density in the continuity equation is neglected. With the p-coordinate, however, the equation that diagnostically determines the "vertical velocity",

$\omega = dp/dt$, is the continuity equation, which has an especially simple form with this coordinate. The θ-coordinate, which is discussed in one of Sadourny's lectures in more detail, is attractive since the coordinate surfaces are material surfaces under adiabatic processes. This eliminates the problem of "differencing" of the vertical advection. Moreover, since there is no mass flux across the coordinate surface under adiabatic processes, the average pressure along an isentropic surface is an invariant. This makes it possible to rigorously define the available potential energy and the gross static stability (see Section 5 of my second lecture) even for a discrete system. Another advantage with the σ-coordinate is that the pressure gradient force is an irrotational vector (when the curl is taken along a constant θ-surface), as in the case where any thermodynamical state variable, such as p, is used as the vertical coordinate. Moreover, the application of a potential vorticity conserving scheme originally developed for the shallow-water equations, such as that of Arakawa and Lamb (1982), gives conservation of (the hydrostatic version of) the Ertel's potential vorticity. With the θ-coordinate, however, the thickness of each layer can become very thin as a front forms. A more serious problem associated with the θ-coordinate would be the case where an isentropic surface becomes vertical.

3. CHARACTERISTICS OF VERTICAL WAVE PROPAGATION IN DIFFERENT VERTICAL GRIDS

Whichever vertical coordinate (possibly except for the θ-coordinate) is used, a proper choice of the vertical grid structure is an important problem in vertical differencing. This is the case even for a quasi-geostrophic system of equations, as is discussed in my second lecture. This problem can be more important in vertical differencing of the primitive equations, the solution of which includes vertically propagating internal gravity waves.

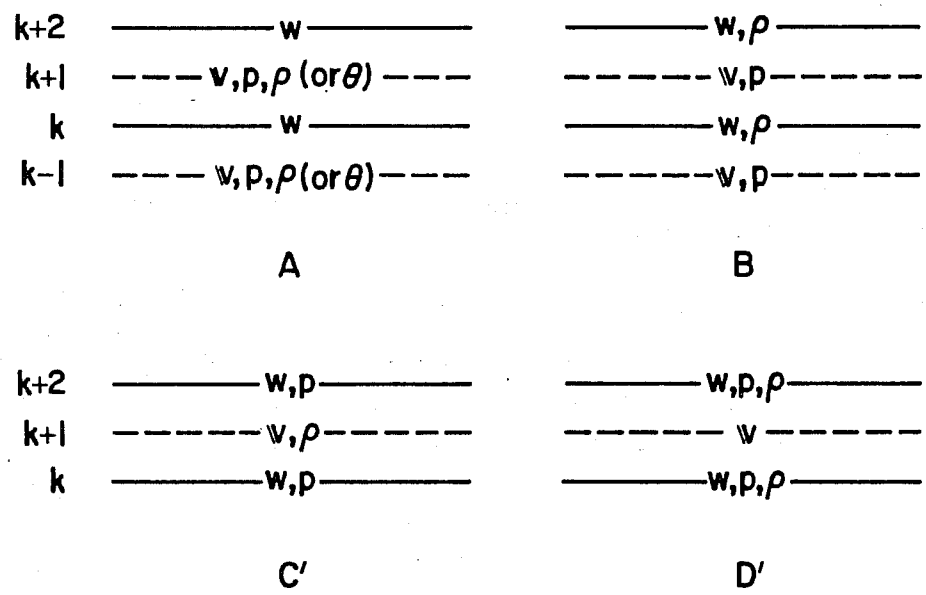

Fig. 2 Four ways of distributing variables over the discrete levels.

Tokioka (1978) compared characteristics of vertical wave propagation in various vertical grids, in which the variables are distributed over the discrete levels differently. The Boussinesq system of equations, linearized with respect to a perturbation on a resting basic state, was used in his analysis. Among the eight possibilities Tokioka considered, the results of the four shown in Fig. 2 will be presented here. In the figure, v is the horizontal velocity, w is the vertical velocity, ρ is the density and p is the pressure.

After separating the three-dimensional equation for w into the horizontal and vertical structure equations, Tokioka obtained the relations between the vertical wavenumber for the continuous case, n, and that for each of the discrete case, N. We have the relation

$$n^2 = \frac{1}{gh}\left(-g\frac{d\ell n\bar{\rho}}{dz}\right) . \tag{1}$$

Here $(-gd\ell n\bar{\rho}/dz)^{1/2}$ is the Brunt-Väisälä frequency of the Boussinesq system, which is assumed to be constant; g is the acceleration due to gravity; and h is the equivalent depth, which is a separation constant introduced in separating the original three-dimensional equations into the horizontal and vertical structure equations. For a forced-wave problem, in which the frequency ν is given, h is determined as an eigenvalue of the horizontal structure equation. We assume here that h, and therefore n, is a given quantity. Using the simplest centered differences for vertical derivatives and the trapezoidal averages wherever needed, he obtained the following results:

Grid A, C', D':

$$N\Delta z = \pm \tan^{-1}\left[\frac{4n\Delta z}{4 - (n\Delta z)^2}\right] . \tag{2}$$

Grid B:

$$N\Delta z = \pm \tan^{-1}\left[\frac{n\Delta z\,\{4 - (n\Delta z)^2\}^{1/2}}{2 - (n\Delta z)^2}\right] . \tag{3}$$

Here Δz is the vertical grid interval, $z_{k+2} - z_k$, and $z_{k+1} = (z_{k+2} + z_k)/2$ has been assumed. These results are plotted in Fig. 3.

With Grids A, C' and D', N is real for all $|n\Delta z|$. Consequently, internal waves in the continuous case ($n^2 > 0$) are also internal waves in the discrete case, regardless of $|n\Delta z|$. This is not the case with Grid B, since N is complex for large $|n\Delta z|$. This can be considered as a demerit of Grid B.

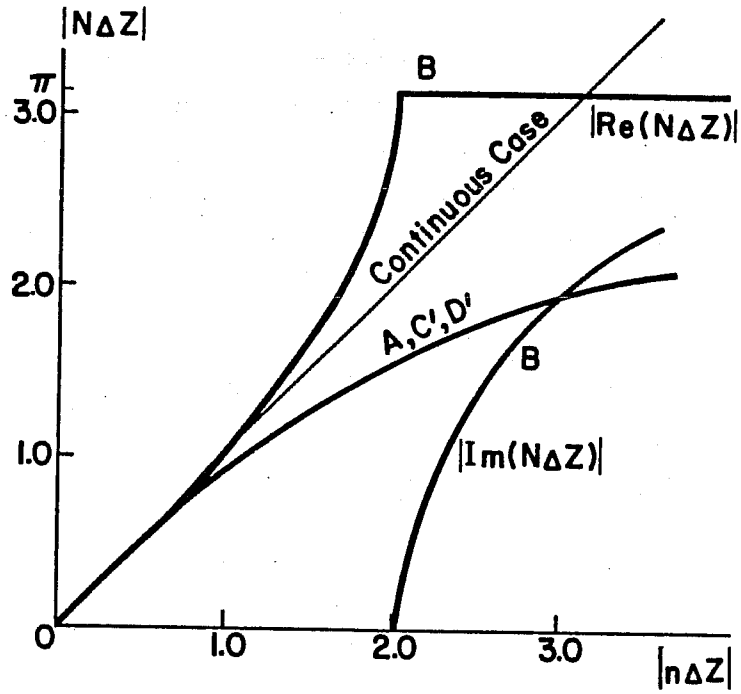

Fig. 3 The relation between $|n\Delta z|$ and $|N\Delta z|$, where n is the vertical wavenumber for the continuous case and N is that for each of the discrete cases. The continuous case is shown by the thin line as a reference. Redrawn from Fig. 2 of Tokioka (1978).

The finite-difference hydrostatic equation for each grid is given by

Grid A:

$$(p'_{k+1} - p'_{k-1})/\Delta z = -\frac{g}{2}(\rho'_{k+1} + \rho'_{k-1}) , \tag{4}$$

Grid B:

$$(p'_{k+1} - p'_{k-1})/\Delta z = -g\,\rho'_{k} , \tag{5}$$

Grid C':

$$(p'_{k+2} - p'_{k})/\Delta z = -g\,\rho'_{k+1} , \tag{6}$$

Grid D':

$$(p'_{k+2} - p'_{k})/\Delta z = -\frac{g}{2}(\rho'_{k+2} + \rho'_{k}) . \tag{7}$$

Here the prime denotes the perturbation.

Based on these forms of the finite-difference hydrostatic equation, Tokioka discussed the possible existence of "computational mode" for each grid. With the grid A, for example, $\rho' \neq 0$ is possible even when $p' = 0$ at all levels, due to the averaging of ρ' in (4). With the grid B, on the other hand, $p' = 0$ at all levels implies $\rho' = 0$, so that there is no "computational mode".

One might argue that there is no "computational mode" with Grid C', since there is no averaging of ρ' in (6). This argument is somewhat misleading, since a pressure perturbation can influence the motion only through the pressure gradient force, which is defined at the levels where velocities are defined. If we follow the trapezoidal rule, as Tokioka used everywhere else, p' that can influence the motion is

$$p'_{k+1} \equiv \frac{1}{2}\,(p'_{k+2} + p'_k), \quad p'_{k-1} \equiv \frac{1}{2}\,(p'_k + p'_{k-2}), \text{ etc.} \tag{8}$$

The hydrostatic equation that governs these p's is

$$(p'_{k+1} - p'_{k-1})/\Delta z = -\frac{g}{2}\,(\rho'_{k+1} + \rho'_{k-1}) \ , \tag{9}$$

which is identical to (4). Fig. 4 shows this situation.

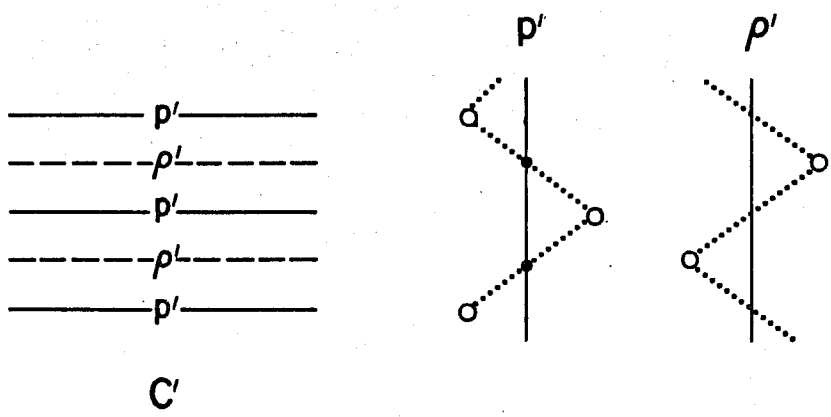

Fig. 4 A possible "computational mode for Grid C'. The open circles show p' and ρ' satisfying (6) and the dots show p' given by (8) satisfying (9).

Note that Grids A and C' correspond to the Lorenz grid and Grid B corresponds to the Charney-Phillips grid referred to in my second lecture. The existence of the "computational mode" is more or less common to any grids of Lorenz-type. It is this situation that is responsible for the difficulty in computing (potential) temperatures from geopotentials given at the same levels, which was pointed out by Phillips (1974).

4. EXAMPLES OF VERTICAL DIFFERENCE SCHEMES FOR THE PRIMITIVE EQUATIONS IN σ-COORDINATES

In spite of some demerits mentioned above, most existing numerical weather prediction and general circulation models with the primitive equations are based on the Lorenz-type grid in σ-coordinates. The principal reason for this is that it is easier with the Lorenz grid to construct a vertical difference scheme that maintains various integral constraints on the continuous system. In this section examples of such schemes will be given.

Arakawa (1972) and (Arakawa and Lamb (1977) chose the following integral constraints in deriving vertical difference schemes:

(I) that the pressure gradient force generate no circulation of vertically integrated momentum along a contour of the surface topography;

(II) that the finite-difference analogues of the energy conversion term have the same form in the kinetic energy and thermodynamic equations;

(III) that the global mass integral of the potential temperature, θ, be conserved under adiabatic processes;

(IV) that the global mass integral of a function of θ, such as θ^2 or $\ell n\theta$, be conserved under adiabatic processes.

Constraint (I) is on the form of the pressure gradient force in the momentum equation, and constraints (III) and (IV) are on the form of the thermodynamic equation. It then follows from constraint (II) that the form of the hydrostatic equation cannot be freely specified. In this way the above four constraints are nearly sufficient to determine the vertical difference scheme, leaving one free to specify only the pressure at which the potential temperature (or the temperature) is carried as a prognostic variable.

Of the four, however, we regard constraints (I) and (II), which involve the pressure gradient force, as the most important in σ-coordinates. If (I) and (II) are not satisfied by the difference equations, an error in the pressure gradient force near steep topography can lead to spurious sources or sinks of the total energy and the circulation of the vertically integrated motion. We will, therefore, first restrict our attention to schemes that satisfy (I) and (II).

For simplicity, we shall use the original σ-coordinate proposed by Phillips (1957) given by

$$\sigma \equiv \frac{p}{p_S} \quad , \tag{10}$$

where p_S is the surface pressure. We then have $\sigma = 0$ for $p = 0$ and $\sigma = 1$ for $p = p_S$.

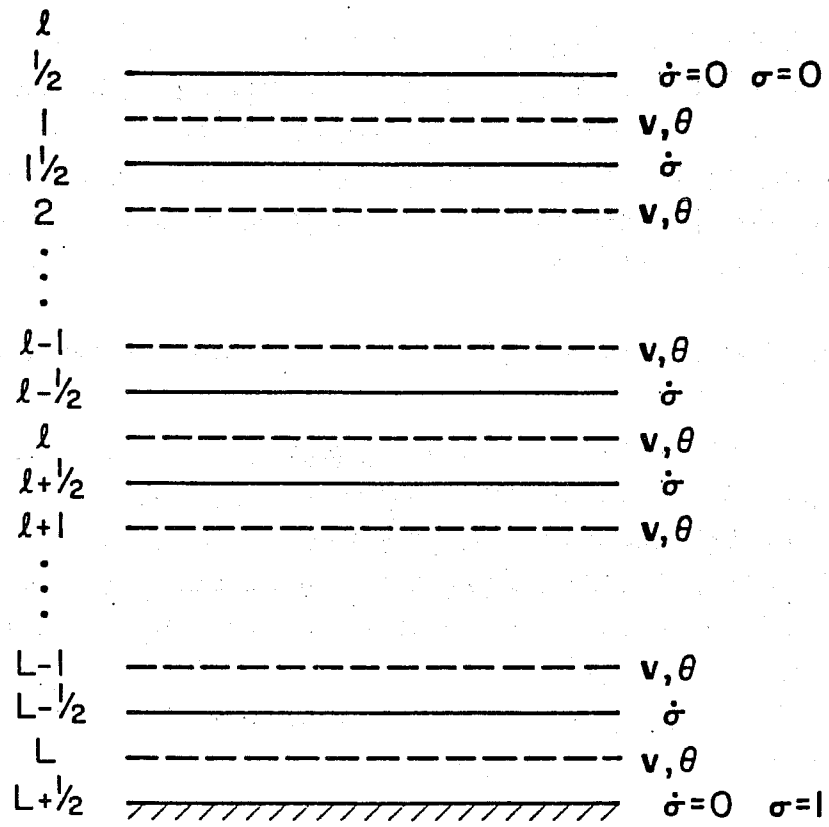

Fig. 5 The structure of the vertically discrete model being considered in this section.

We now consider a Lorenz-type grid shown by Fig. 5. In the following, details in deriving equations, which can be found in Arakawa and Suarez (1983), will be omitted.

A discrete form of the continuity equation for the σ-coordinate defined by (10) is given by

$$\frac{\partial p_S}{\partial t} + \nabla\cdot(p_S \mathbf{v}_\ell) + \left[\frac{\delta(p_S\dot{\sigma})}{\delta\sigma}\right]_\ell = 0 . \tag{11}$$

Here and hereafter, δA for an arbitrary variable A is defined by

$$(\delta A)_\ell \equiv \hat{A}_{\ell+\frac{1}{2}} - \hat{A}_{\ell-\frac{1}{2}} , \tag{12}$$

where a caret is used for variables at half-integer levels in Fig. 5. We begin by writing the pressure gradient force as

$$-(\nabla_p\phi)_\ell = -\frac{1}{p_S}\nabla(p_S\phi_\ell) + \frac{1}{p_S}\left[\frac{\delta(\sigma\phi)}{\delta\sigma}\right]_\ell \nabla p_S . \tag{13}$$

We can then show

$$\sum_{\ell=1}^{L} (p_S \delta\sigma)_\ell (-\nabla_p \phi)_\ell = -\nabla \left[\sum_{\ell=1}^{L} (p_S \phi \delta\sigma)_\ell - \phi_S p_S \right] - p_S \nabla \phi_S \,, \tag{14}$$

which means that constraint (I) is satisfied.

Evaluating the work done by the pressure gradient force given by (13), we find that total energy is conserved if the discrete form of the thermodynamic equation has the form

$$\begin{aligned} \frac{\partial}{\partial t}(p_S c_p T_\ell) + \nabla\cdot(p_S \mathbf{v}_\ell c_p T_\ell) + \left[\frac{\delta(p_S \dot{\sigma} c_p T)}{\delta\sigma}\right]_\ell \\ = \left[\phi - \frac{\delta(\sigma\phi)}{\delta\sigma}\right]_\ell \left(\frac{\partial}{\partial t} + \mathbf{v}_\ell\cdot\nabla\right) p_S \\ + \frac{1}{(\delta\sigma)_\ell}\left[(p_S\dot{\sigma})_{\ell+\frac{1}{2}}(\phi_\ell - \hat{\phi}_{\ell+\frac{1}{2}}) + (p_S\dot{\sigma})_{\ell-\frac{1}{2}}(\hat{\phi}_{\ell-\frac{1}{2}} - \phi_\ell)\right] . \end{aligned} \tag{15}$$

We must now choose a discrete form of the hydrostatic equation. Its continuous form is given by

$$\frac{\partial\phi}{\partial p} = -\alpha \tag{16}$$

or, more generally,

$$\frac{\partial\phi}{\partial f} = -\frac{RT}{pdf/dp} \,, \tag{17}$$

where f is a function of p only. One way of deriving a discrete form of (17) is to assume that layer ℓ, which is the layer bounded by levels $\ell - \frac{1}{2}$ and $\ell + \frac{1}{2}$, is a layer of constant RT/(pdf/dp). Then, by integrating (17), we obtain

$$\hat{\phi}_{\ell-\frac{1}{2}} - \phi_\ell = \left(\frac{RT}{pdf/dp}\right)_\ell (f_\ell - \hat{f}_{\ell-\frac{1}{2}}) \tag{18}$$

$$\phi_\ell - \hat{\phi}_{\ell+\frac{1}{2}} = \left(\frac{RT}{pdf/dp}\right)_\ell (\hat{f}_{\ell+\frac{1}{2}} - f_\ell) \,. \tag{19}$$

Elimination of ϕ_ℓ between (18) and (19) gives

$$\hat{\phi}_{\ell-\frac{1}{2}} - \hat{\phi}_{\ell+\frac{1}{2}} = \left(\frac{RT}{pdf/dp}\right)_\ell (\hat{f}_{\ell+\frac{1}{2}} - \hat{f}_{\ell-\frac{1}{2}}) \,. \tag{20}$$

Eliminating the common factor in the right hand sides of (18) and (19), on the other hand, we obtain

$$\phi_\ell = \frac{(\hat{f}_{\ell+\frac{1}{2}} - f_\ell)\hat{\phi}_{\ell-\frac{1}{2}} + (f_\ell - f_{\ell-\frac{1}{2}})\hat{\phi}_{\ell+\frac{1}{2}}}{\hat{f}_{\ell+\frac{1}{2}} - \hat{f}_{\ell-\frac{1}{2}}} , \tag{21}$$

which shows that ϕ_ℓ is a weighted mean of $\hat{\phi}_{\ell-\frac{1}{2}}$ and $\hat{\phi}_{\ell+\frac{1}{2}}$. Increasing ℓ in (18) by one and adding the result to (19), we obtain

$$\phi_\ell - \phi_{\ell+1} = (\frac{RT}{pdf/dp})_{\ell+1}(f_{\ell+1} - \hat{f}_{\ell+\frac{1}{2}}) + (\frac{RT}{pdf/dp})_\ell(\hat{f}_{\ell+\frac{1}{2}} - f_\ell) . \tag{22}$$

It should be noted that the forms (20) and (22) correspond to (6) and (9) for Grid C', respectively.

At each half-integer level, $\hat{\sigma}$ is prescribed, and therefore $\hat{p}$ and $\hat{f}$ there can be determined for a given p_S. It then remains to determine f at integer levels to obtain a complete vertical differencing. We may choose

$$f_\ell \equiv \frac{1}{\hat{p}_{\ell+\frac{1}{2}} - \hat{p}_{\ell-\frac{1}{2}}} \int_{\hat{p}_{\ell-\frac{1}{2}}}^{\hat{p}_{\ell+\frac{1}{2}}} f dp . \tag{23}$$

Motivation for this choice is given in Arakawa and Suarez (1983).

A member of the family of schemes presented in this section is the scheme proposed by Simmons and Burridge (1981), which can be obtained by choosing f = ℓnp. Then

$$(\frac{RT}{pdf/dp})_\ell = RT_\ell . \tag{24}$$

Another member of this family of schemes is the scheme proposed by Arakawa and Suarez (1983), which can be obtained by choosing f = P, where

$$P \equiv (\frac{p}{p_o})^\kappa . \tag{25}$$

Then

$$(\frac{RT}{pdf/dp})_\ell = c_p\theta_\ell , \tag{26}$$

where θ_ℓ is the potential temperature for the layer ℓ defined by

$$\theta_\ell \equiv \frac{T_\ell}{P_\ell} . \tag{27}$$

With this choice the discrete thermodynamic equation (15) can be rewritten as

$$\frac{\partial}{\partial t}(p_S\theta_\ell) + \nabla\cdot(p_S v_\ell \theta_\ell) + \left[\frac{\delta(p_S\dot{\sigma}\theta)}{\delta\sigma}\right]_\ell = 0 \tag{28}$$

with $\hat{\theta}$ defined by

$$\hat{\theta}_{\ell+\frac{1}{2}} = \frac{(P_{\ell+1} - \hat{P}_{\ell+\frac{1}{2}})\theta_{\ell+1} + (\hat{P}_{\ell+\frac{1}{2}} - P_{\ell})\theta_{\ell}}{P_{\ell+1} - P_{\ell}} \tag{29}$$

The discrete thermodynamic equation (28) satisfies constraint (III).

Arakawa (1972) and Arakawa and Lamb (1977) showed that the use of

$$\hat{\theta}_{\ell+\frac{1}{2}} = \frac{(F'_{\ell+1}\theta_{\ell+1} - F_{\ell+1}) - (F'_{\ell}\theta_{\ell} - F_{\ell})}{F'_{\ell+1} - F'_{\ell}} , \tag{30}$$

instead of (29), satisfies constraint (IV). With $F(\theta) \equiv \theta^2$, (30) gives

$$\hat{\theta}_{\ell+\frac{1}{2}} = \frac{1}{2}(\theta_{\ell+1} + \theta_{\ell}). \tag{31}$$

This was chosen by Lorenz (1960) for the balanced system of equations and by Arakawa (1972) for the primitive equations. Arakawa and Lamb (1977), on the other hand, chose $F(\theta) \equiv \ell n\theta$. Eq. (30) then gives

$$\hat{\theta}_{\ell+\frac{1}{2}} = \frac{\ell n\ \theta_{\ell} - \ell n\ \theta_{\ell+1}}{1/\theta_{\ell+1} - 1/\theta_{\ell}} . \tag{32}$$

The advantage of this choice for the stratosphere was discussed by Arakawa and Lamb (1977) (see Section V.A.4 of their paper) from the point of view of a constraint on the statistical distribution of θ, and by Tokioka (1978) (see also Arakawa and Lamb, 1977, Section V.C.2) from the point of view of wave propagation through an isothermal atmosphere. These schemes, however, do not belong to the family of schemes described in this section. In particular, the discrete form of the hydrostatic equation cannot be written in the form of (20). This can be considered as a demerit of the schemes that satisfy all of the constraints (I) through (IV). For example, in actual numerical weather predictions with a scheme that is a member of the family presented in this section, we may use (20) for initializing model's (potential) temperatures from the observed values of ϕ at half-integer levels. With a scheme that uses (30), however, there is no such simple relationship as (20), and therefore we must initialize the model's (potential) temperatures from the observed values of ϕ at integer levels, using a relationship analogous to (22). Since an average of the temperatures at two adjacent integer levels appears in such a relationship, as in the right hand side of (22), we usually obtain temperatures highly oscillating from level to level, as Phllips (1974) pointed out.

5. LAYER-MODELING VS. INTERPOLATION APPROACHES

The family of schemes presented in the last section are constructed following an approach which may be called "layer-modeling". In this approach prognostic variables (other than the surface pressure) are defined for each sub-layer bounded by adjacent solid lines in Fig. 5, rather than for each discrete level. The finite-difference schemes for the continuity, momentum and thermodynamic equations are then constructed to represent the budgets of mass, momentum and enthalpy (or potential enthalpy) for each sub-layer. Here we are assuming, either explicitly or implicitly, that the prognostic variables are piecewise constant within each sub-layer. The value of a prognostic variable at an interface of two sub-layers, which is necessary for calculating the vertical flux of that variable through the interface, can be determined by placing further integral constraints. In the examples given in the last section, furthermore, the discrete hydrostatic equation is constructed by assuming that the quantity RT/(pdf/dp) is piecewise constant, as shown schematically by the heavy solid lines in Fig. 6(a).

Another way of constructing finite-difference schemes may be called "interpolation approach". In this approach priority is given to local accuracy, without explicit considerations on the budgets and other integral constraints. Vertical discretization is made using interpolations from directly predicted values, shown by the solid circles in Fig. 6(a). The hydrostatic equation can be discretized by assuming that a thermodynamic variable is, for example, piecewise linear as shown schematically by the heavy dashed lines in Fig. 6(a).

The difference between these two approaches can be seen most clearly in (29). Suppose that the thickness of layer $\ell+1$, measured by P, is much smaller than that of layer ℓ, as shown in Fig. 6(b). Eq. (29) then shows that $\hat{\theta}_{\ell+\frac{1}{2}}$ is mainly determined by θ_{ℓ}, as shown by the solid triangle in the figure. $\hat{\theta}_{\ell+\frac{1}{2}}$ obtained by an interpolation, on the other hand, is mainly determined by $\theta_{\ell+1}$ under such a situation, as shown by the open triangle in the figure.

While finite-difference schemes constructed following the "layer-modeling" are more attractive, the above example shows that they can have poor local accuracy when the vertical spacing of the sub-layers is very uneven. This indicates that the choice of a proper vertical spacing is as important as design of the vertical difference-scheme itself.

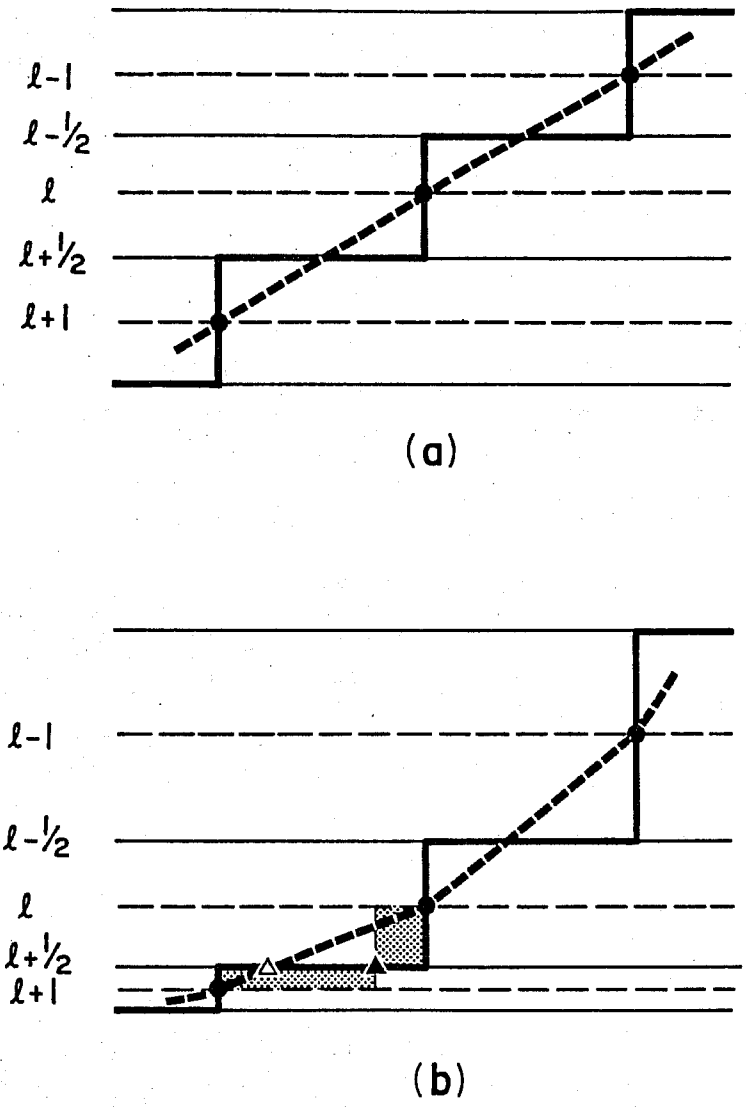

Fig. 6 Schematic figures showing the difference between the "layer-modeling" (heavy solid lines) and "interpolation" (heavy dashed lines) approaches. See text for explanation.

6. VERTICAL STRUCTURE OF FREE OSCILLATIONS

The existence of an artificial upper boundary in numerical weather prediction models can be a serious problem. By comparing solutions of the tidal equation for infinite and bounded atmospheres, Lindzen et al. (1968) showed that applying the upper boundary condition dp/dt = 0 at some finite height introduces spurious free oscillations and correspondingly spurious resonances of forced oscillations. They also pointed out that having the model top at p = 0 is in practice equivalent to having the model top at some small finite p due to inevitable finite-difference errors. This latter point, in particular, is supported by later studies by Nakamura (1976) and Kirkwood and Derome (1977).

We have made an eigenvalue analysis of a discrete version of the vertical structure of various free oscillations and the "computational mode" in a discrete model. In this analysis, the Arakawa-Suarez scheme described in the last section, was used with a modified definition of σ given by $\sigma \equiv (p - p_T)/(p_S - p_T)$. Here p_T is the pressure at the model top, which is assumed to be a material surface so that $\dot{\sigma} = 0$ there. In the results shown below, p_T = 100 mb was used.

Fig. 7 shows the vertical structure of the "computational modes" in 7-layer and 14-layer models, with different spacing between the half-integer levels. Here a "computational mode" is defined by the vertical structure for which the pressure gradient force, which is defined at integer levels, is zero for all layers. The scale of the horizontal axis of Fig. 7 is such that a single unit corresponds to 1°C of potential temperature perturbation when the surface pressure perturbation is 0.1 mb.

Fig. 8 shows the 7th eigenmode of the 7-layer and 14-layer models, which is the highest vertical mode in the 7-layer model. An equal spacing in $\ell n p$ between half-integer levels is used. The scale of the horizontal axis of θ perturbation is such that a single unit corresponds to 1°C of the potential temperature perturbation when a single unit of the horizontal axis of the "height" perturbation is 1 m. Here the height means the height of an isobaric surface, rather than that of a sigma surface.

Fig. 9 is the same as Fig. 8 except for the highest mode in the 14-layer model.

Fig 10 shows the speed of pure gravity waves for each mode in the 7-layer and 14-layer models.

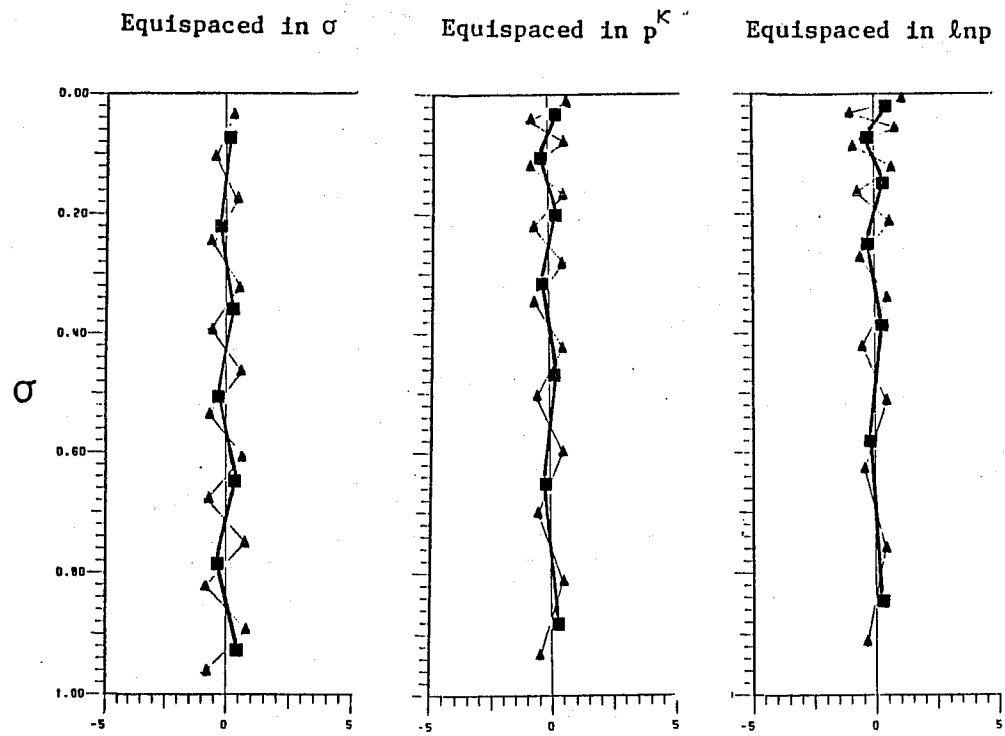

Fig. 7 The amplitude of θ for computational mode in 7-layer (shown by solid squares) and in 14-layer (shown by solid triangles) models, with three different types of spacing between half-integer levels.

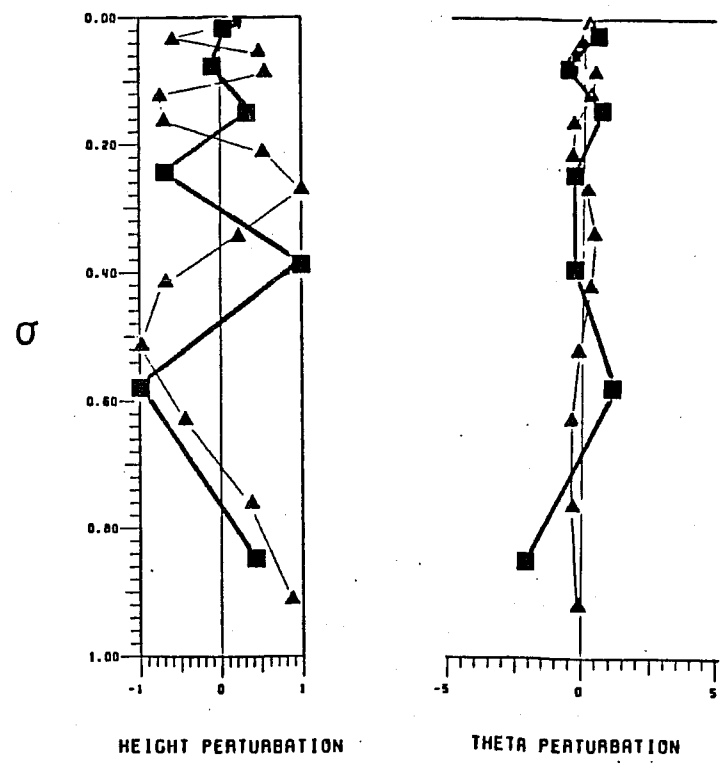

Fig. 8 See text for explanation.

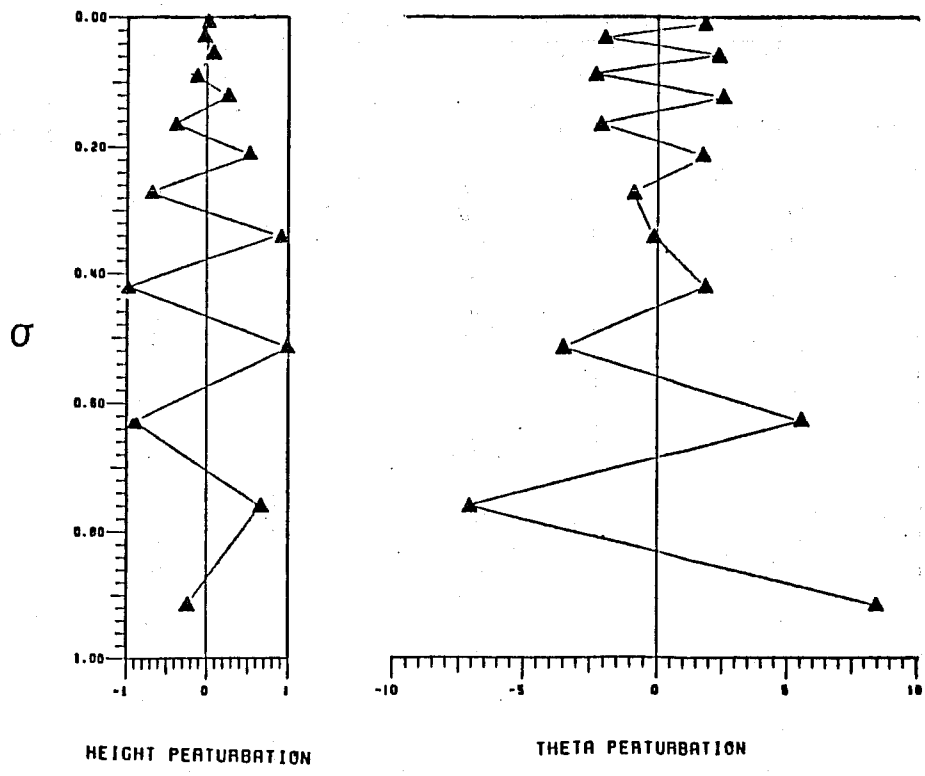

Fig. 9 See text for explanation.

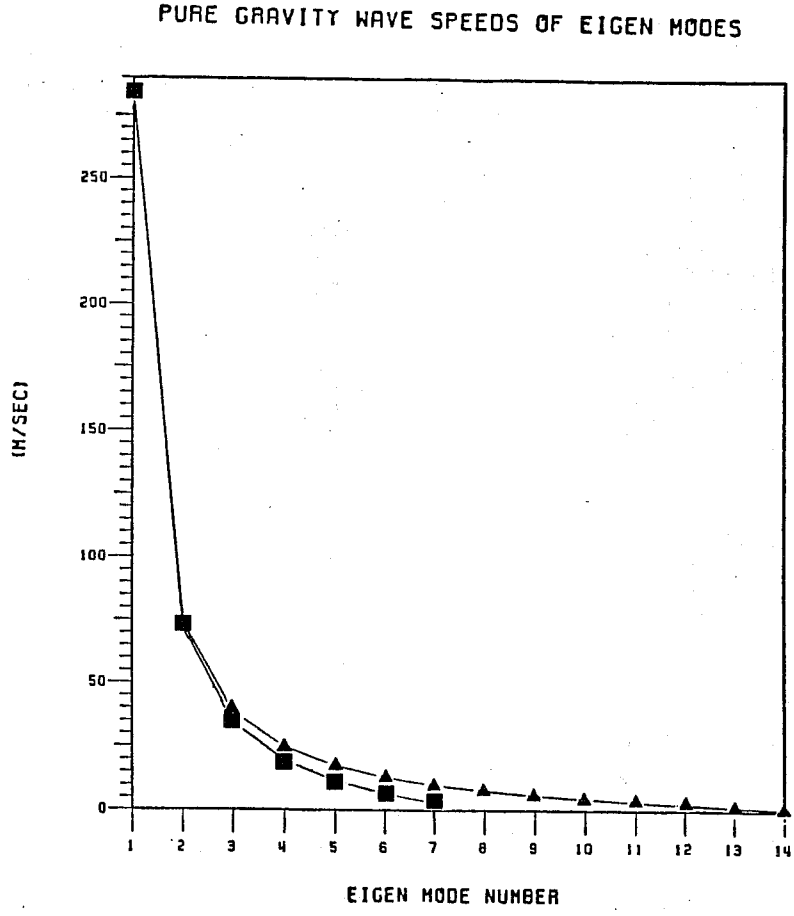

Fig. 10 Speed of pure gravity waves in the 7-layer and 14-layer models for each eigenmode.

This type of analysis, which is similar to that of Williamson and Dickinson (1976), has been extended with a multi-layer model with the top at 1 mb. The result shows very large (relative) amplitude in temperature perturbation near the top for high vertical modes due to false reflection of vertically-propagating waves. Treating the upper boundary condition properly in a numerical weather prediction model is, therefore, an important problem in vertical discretization of the primitive equations.

References

Arakawa, A., 1972: Design of the UCLA general circulation model. Numerical Simulation of Weather and Climate, Tech. Rep. No. 7, Dept. Meteor., UCLA, Los Angeles, CA 90024.

Arakawa, A., and V.R. Lamb, 1977: Computational design of the basic dynamical processes of the UCLA general circulation model. Methods in Computational Physics, Vol. 17, J. Chang, Ed., Academic Press, 337 pp.

Arakawa , A., and M.J. Suarez, 1983: Vertical differencing of the primitive equations in sigma coordinates. Mon. Wea. Rev., 111, 34-45.

Kasahara, A., 1974: Various vertical coordinate systems used for numerical weather prediction. Mon. Wea. Rev., 102, 509-522.

Kirkwood, E., and J.F. Derome, 1977: Some effects of the upper boundary condition and vertical resolution on modeling forced, stationary, planetary waves. Mon. Wea. Rev., 105, 1239-1312.

Lindzen, R.S., E.S. Batten and J.W. Kim, 1968: Oscillations in atmospheres with tops. Mon. Wea. Rev., 96, 133-140.

Nakamura, H., 1978: Dynamical effects of mountains on the general circulation of the atmosphere: I. Development of finite-difference schemes suitable for incorporating mountains. J. Meteor. Soc. Japan, 56, 317-339.

Phillips, N.A., 1957: A coordinate system having some special advantages for numerical forecasting. J. Meteor., 14, 184-185.

Phillips, N.A., 1974: Application of Arakawa's energy-conserving layer model to operational numerical weather prediction. Office Note 104, National Meteorological Center, NWS/NOAA, Washington, D.C., 20233, 40 pp.

Sunqvist, H., 1979: Vertical coordinates and related discretization. Numerical methods used in atmospheric models, Vol II. Garp Publication Series No. 17, 1-50.

Simmons, A.J., and D.M. Burridge, 1981: An energy and angular momentum conserving vertical finite-difference scheme and hybrid vertical coordinates. Mon. Wea. Rev., 109, 758-766.

Tokioka, T., 1978: Some consideration on vertical differencing. J. Meteor. Soc. Japan, 56, 98-111.

Williams, D.L., and R.E. Dickinson, 1976: Free oscillations of the NCAR global circulation model. Mon. Wea. Rev., 104, 1372-1391.